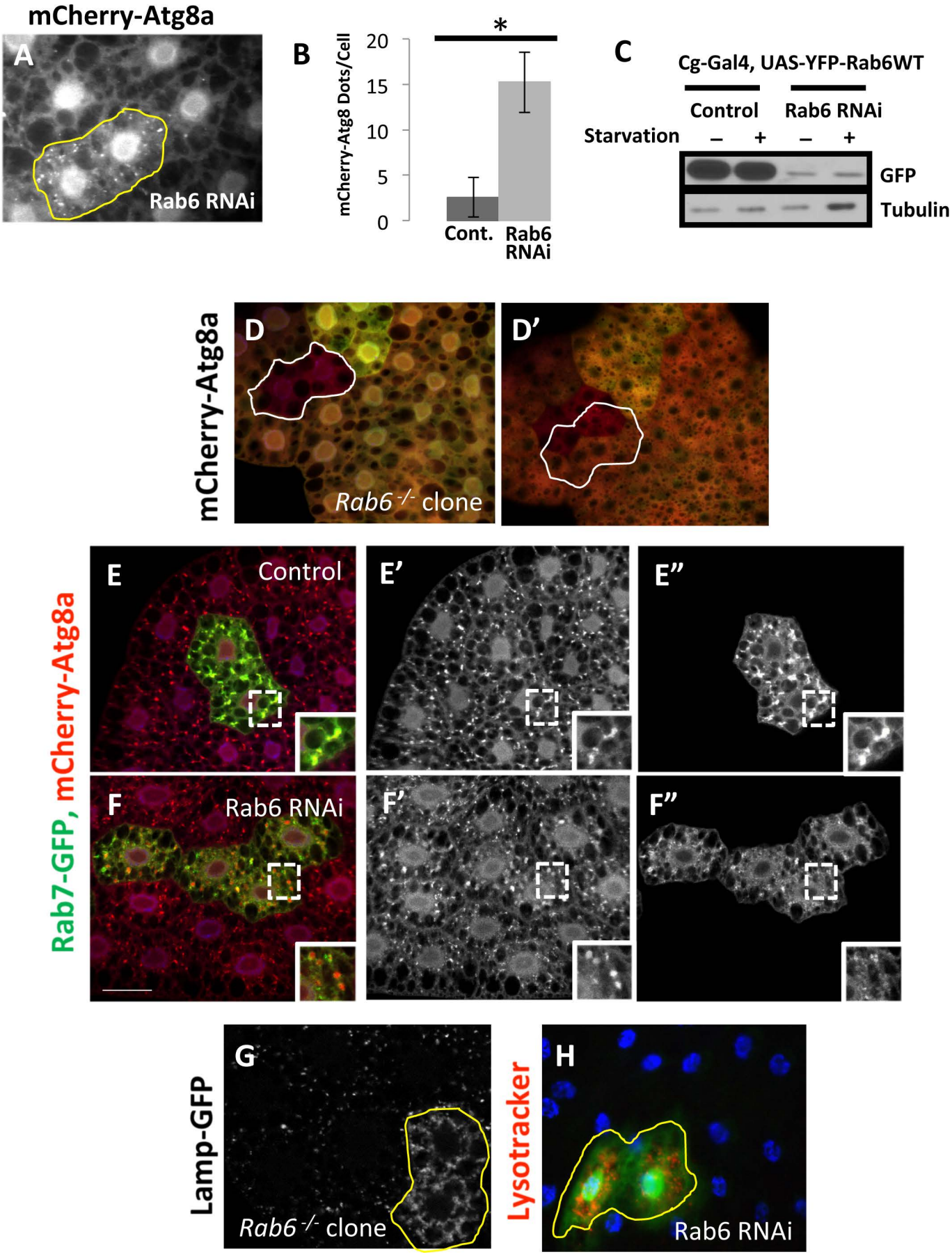
mCherry-Atg8a
A
Rab6 RNAi
B
mCherry-Atg8 Dots/Cell
20
15
10
5
0
*
Cont.
Rab6 RNAi
C
Cg-Gal4, UAS-YFP-Rab6WT
Control
Rab6 RNAi
Starvation
– + – +
GFP
Tubulin
mCherry-Atg8a
D
Rab6 -/- clone
D'
Rab7-GFP, mCherry-Atg8a
E
Control
E'
E''
F
Rab6 RNAi
F'
F''
Lamp-GFP
G
Rab6 -/- clone
Lysotracker
H
Rab6 RNAi

Figure S1. Loss of Rab6 leads to expansion of the lysosomal compartment and accumulation of autolysosomes.

A) Representative image of larval fat body containing a *Rab6* RNAi expressing cell clone (outlined in yellow), showing increased accumulation of mCherry-Atg8a-marked autophagic vesicles relative to surrounding control cells under fed conditions.

B) Mean number of mCherry-Atg8a punctate per cell in control (yw) and Rab6-depleted fat bodies is indicated. n=20 clones and 10 larvae analyzed per genotype. *p<0.05, Student's t-test. Error bars indicate standard error of the mean (s.e.m.).

C) YFP-Rab6 is reduced in extracts of Rab6-depleted fat body tissue under basal and starved conditions as compared to control fat body tissue. YFP-Rab6 was detected via western blot using a GFP antibody.

D) Representative images of larval fat body containing a *Rab6* null cell clone (outlined in white), showing absence of mCherry-Atg8a-marked autophagic vesicles similar to surrounding control cells under fed conditions in early L3 instar larvae. Nuclear (D) and cortical (D') focal planes are shown.

E,F) Representative image of larval fat body containing a control (E) or *Rab6* RNAi expressing (F) cell clone marked by expression of Rab7-GFP, under starvation conditions. mCherry-Atg8a-marked autophagic vesicles co-localize with Rab7-GFP under both conditions. E'-F') and E"-F") depict red and green channels, respectively for better visualization.

G) Representative image of larval fat body containing a *Rab6* null cell clone (outlined in yellow), showing expansion of Lamp-GFP labeled lysosomes relative to surrounding control cells under fed conditions.

H) Representative image of larval fat body containing a *Rab6* RNAi expressing cell clone (marked by GFP), showing increased accumulation of Lysotracker Red autolysosomes relative to surrounding control cells under fed conditions.

Scale bar, 25μm. Genotypes: A) *hs-flp; UAS-Dicer/+; r4-mCherry-Atg8a, Act<CD2<Gal4, UAS-GFP /UAS-Rab6-dsRNA.* C) *Control: Cg-Gal4, UAS-Rab6-WT-YFP/+; +/+. Rab6 RNAi: Cg-Gal4, UAS-Rab6-WT-YFP/+; UAS_Rab6-dsRNA/+.* D) *hs-flp; Rab6^{D23D}, FRT40A /UAS-2x-eGFP, FRT40A, fb-Gal4; UAS-mCherry-Atg8a/+.* E) *hs-flp; UAS-Rab7-GFP/+; r4-mCherry-Atg8a, Act<CD2<Gal4, /+.* F) *hs-flp; UAS-Rab7-GFP/+; r4-mCherry-Atg8a, Act<CD2<Gal4, /+.* G) *hs-flp; Rab6^{D23D}, FRT40A /UAS-ds-Red, FRT40A, fb-Gal4, UAS-Lamp-GFP; +/+.* H) *hs-flp; +/+; Act<CD2<Gal4, UAS-GFP/UAS-Rab6-dsRNA*

Journal of Cell Science • Supplementary information

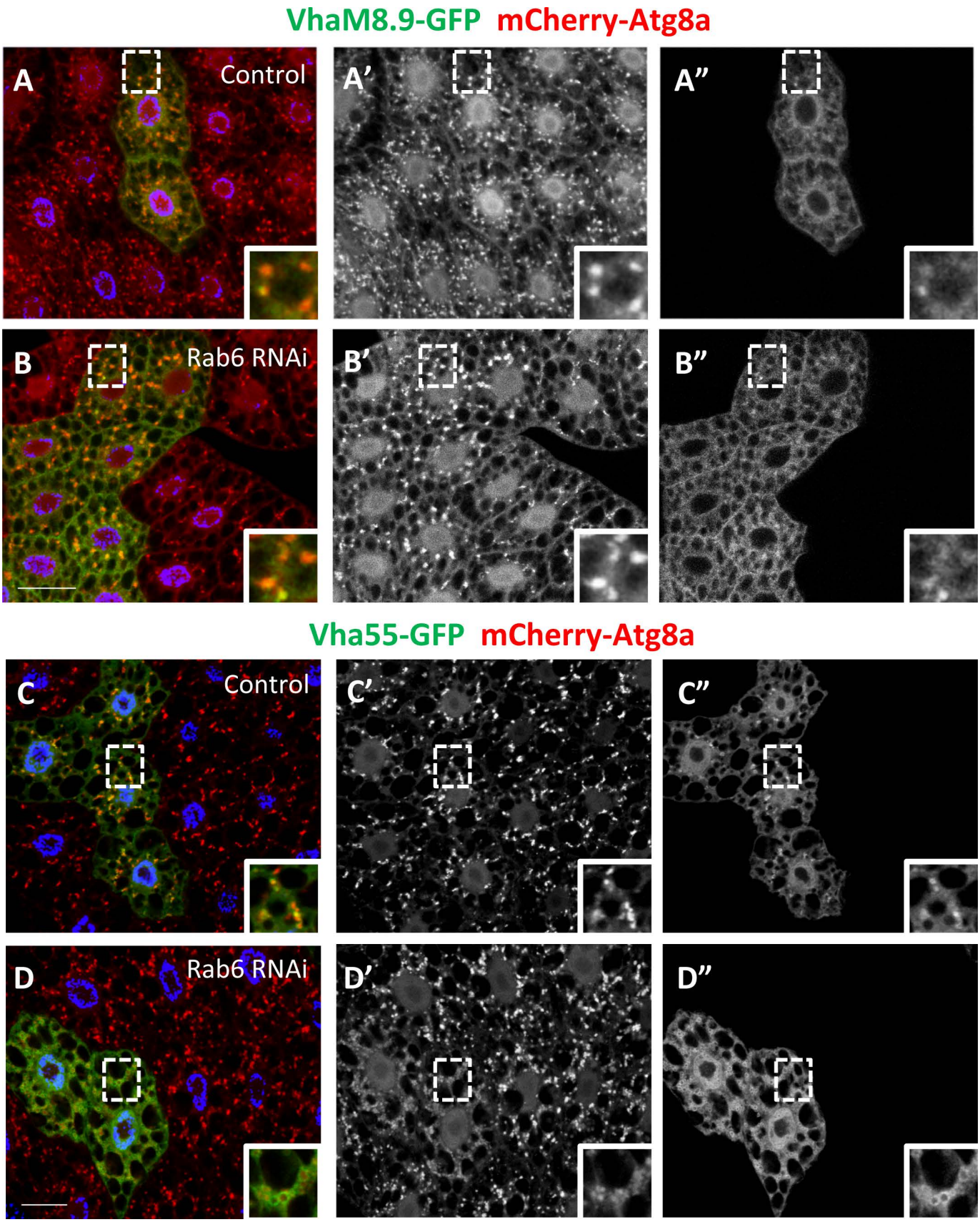

Journal of Cell Science • Supplementary information

Figure S2. Rab6 is not required for the recruitment of vacuolar ATPases to autophagic vesicles.

Representative images of larval fat body containing a control (A,C) or *Rab6* RNAi expressing (B,D) cell clone marked by expression of Vha8.9-GFP (A,B) or Vha55-GFP (C,D), under starvation conditions. mCherry-Atg8a-marked autophagic vesicles co-localize with v-ATPase subunits in both control and Rab6 depleted cells. mCherry (‘) and GFP (“) channels are shown separately in grayscale.

Scale bar, 25µm. Genotypes: A) *hs-flp; UAS-VhaM8.9-GFP/+; r4-mCherry-Atg8a, Act<CD2<Gal4, /+.* B) *hs-flp; UAS-VhaM8.9-GFP/+; r4-mCherry-Atg8a, Act<CD2<Gal4/UAS-Rab6-dsRNA.* C) *hs-flp; UAS-Vha55-GFP/+; r4-mCherry-Atg8a, Act<CD2<Gal4/+.* D) *hs-flp; UAS-Vha55-GFP/+; r4-mCherry-Atg8a, Act<CD2<Gal4/UAS-Rab6-dsRNA*

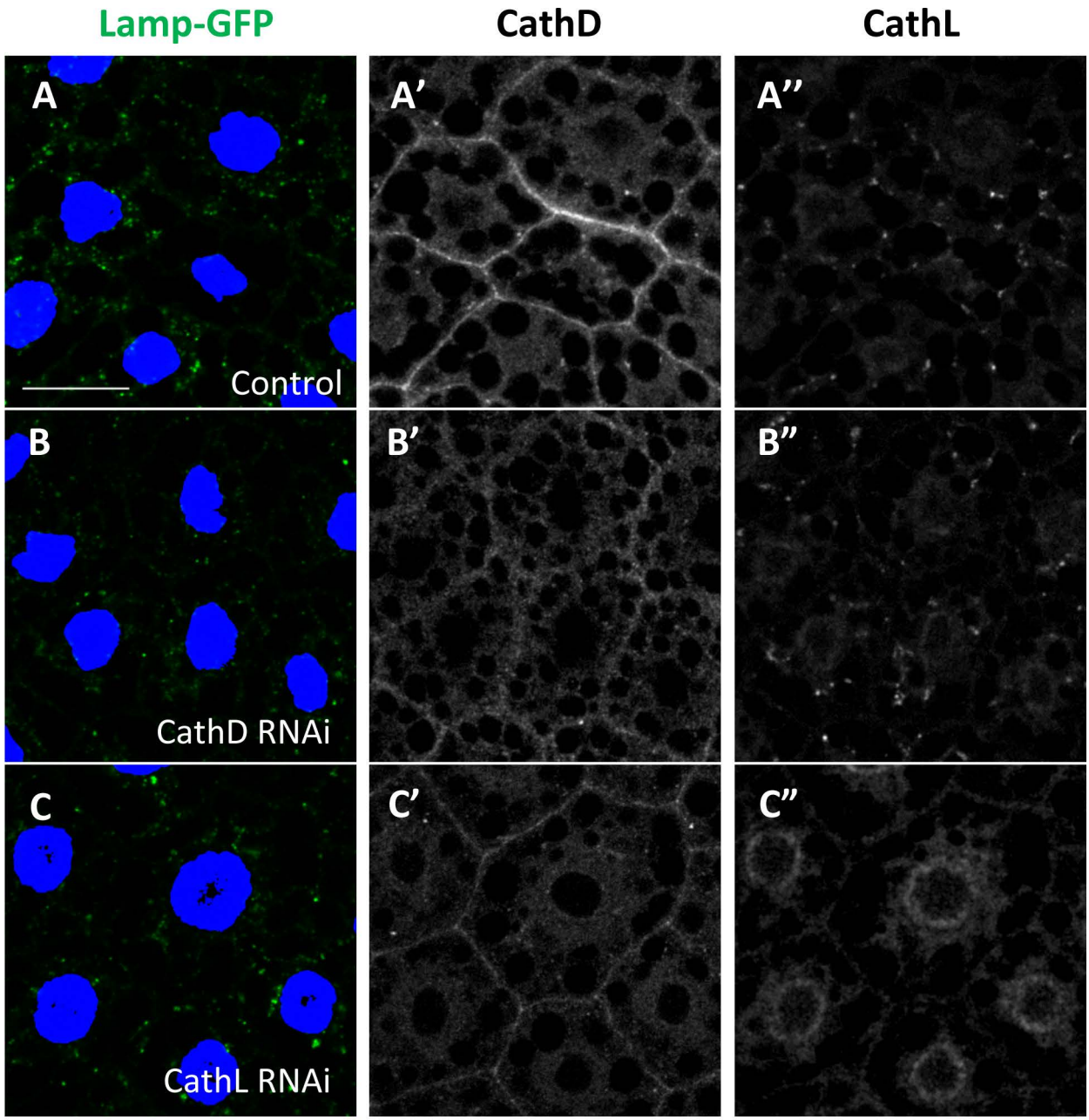

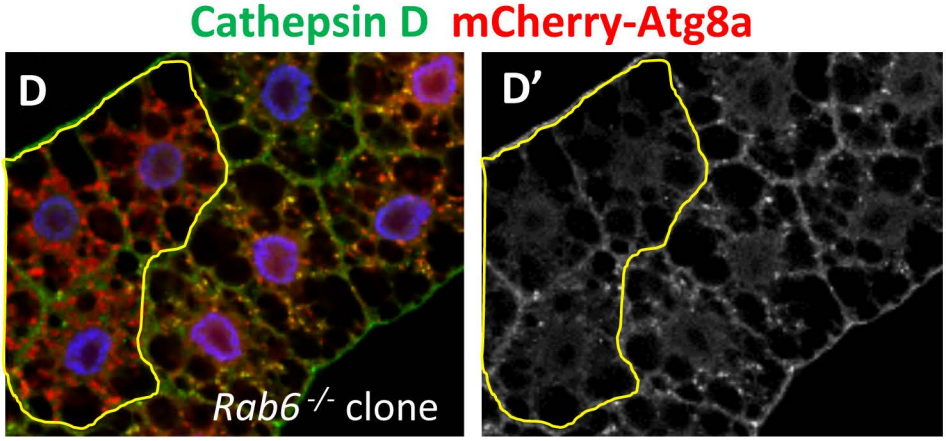

Figure S3. Cathepsin D and Cathepsin L localize to autolysosomes dependent on Rab6.

A-C) RNAi-mediated depletion of Cathepsin D (B) and Cathepsin L (C) throughout the larval fat body results in reduction of Cathepsin D (B') and Cathepsin L (C") staining from punctae that co-localize with the lysosomal compartment marker Lamp-GFP. Nuclei are marked by DAPI (blue).

D) Autolysosomal Cathepsin D staining (green) is reduced in Rab6 null cell clones (outlined in yellow). Cathepsin D staining is depicted in grayscale in (D'). 4hr starvation conditions.

Scale bar, 25μm. Genotypes: A) *Cg-Gal4 UAS-Lamp-GFP/+*. B) *Cg-Gal4 UAS-Lamp-GFP/UAS-CathD-dsRNA*. C) *Cg-Gal4 UAS-Lamp-GFP/UAS-CathL-dsRNA*. D) *hs-flp; Rab6^{D23D}, FRT40A /UAS-2x-eGFP, FRT40A, fb-Gal4; UAS-mCherry-Atg8a/+*.

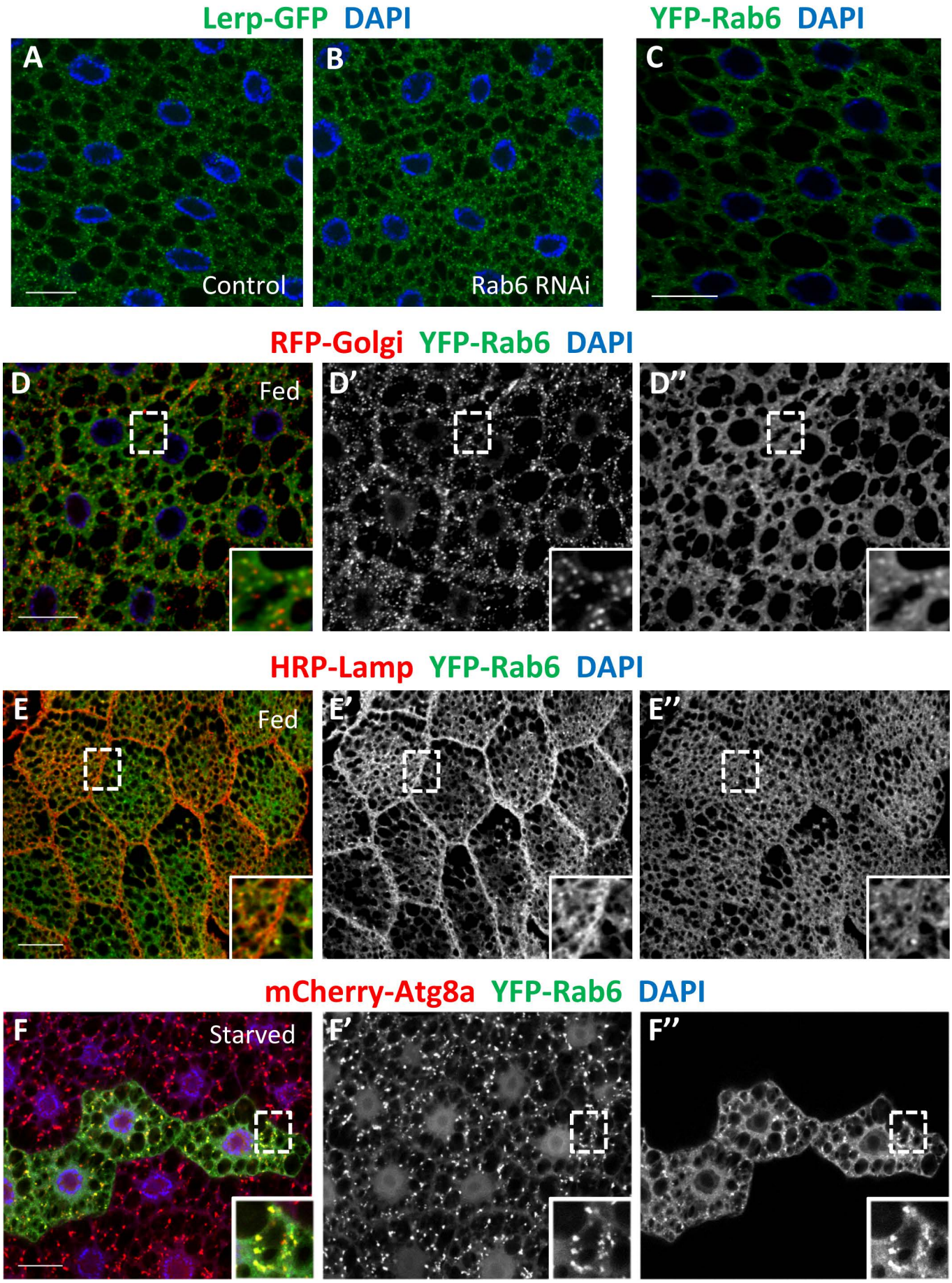

Journal of Cell Science • Supplementary information

Figure S4. Rab6 localizes to distinct subcellular compartments and is not required for LERP localization in fat body cells.

A,B) Lerp-GFP displays a similar punctate localization in control (A) and Rab6-depleted (B) fat body cells; fed conditions.

C) Representative image of larval fat body showing cytoplasmic distribution of YFP-Rab 6 under fed conditions.

D) Co-localization of YFP-Rab6 and RFP-Golgi expressed throughout the larval fat body under fed conditions. D',D") depict red and green channels, respectively, for better visualization.

E) Co-localization of YFP-Rab6 and HRP-Lamp expressed throughout the larval fat body under fed conditions. HRP antigen was visualized by immunostaining. E', E") depict red and green channels, respectively, for better visualization.

F) Representative image of larval fat body containing a cell clone marked by expression of YFP-Rab6, showing formation of punctae under starvation conditions that colocalize with mCherry-Atg8a-marked autophagic vesicles under 4hr starvation conditions. F', F") depict red and green channels, respectively, for better visualization.

Scale bar, 25μm. Genotypes: A,B) *control*: *Cg-Gal4/Tubulin-Lerp-GFP. Rab6 RNAi: Cg-Gal4/Tubulin-Lerp-GFP; UAS-Rab6-dsRNA/+.* C) *Cg-Gal4 UAS-YFP-Rab6.* D) *Cg-Gal4 UAS-YFP-Rab6/UAS-RFP-Golgi.* E) *Cg-Gal4 UAS-YFP-Rab6/UAS-HRP-Lamp.* F) *hs-flp; UAS-YFP-Rab6/+; r4-mCherry-Atg8a, Act<CD2<Gal4, /+.*

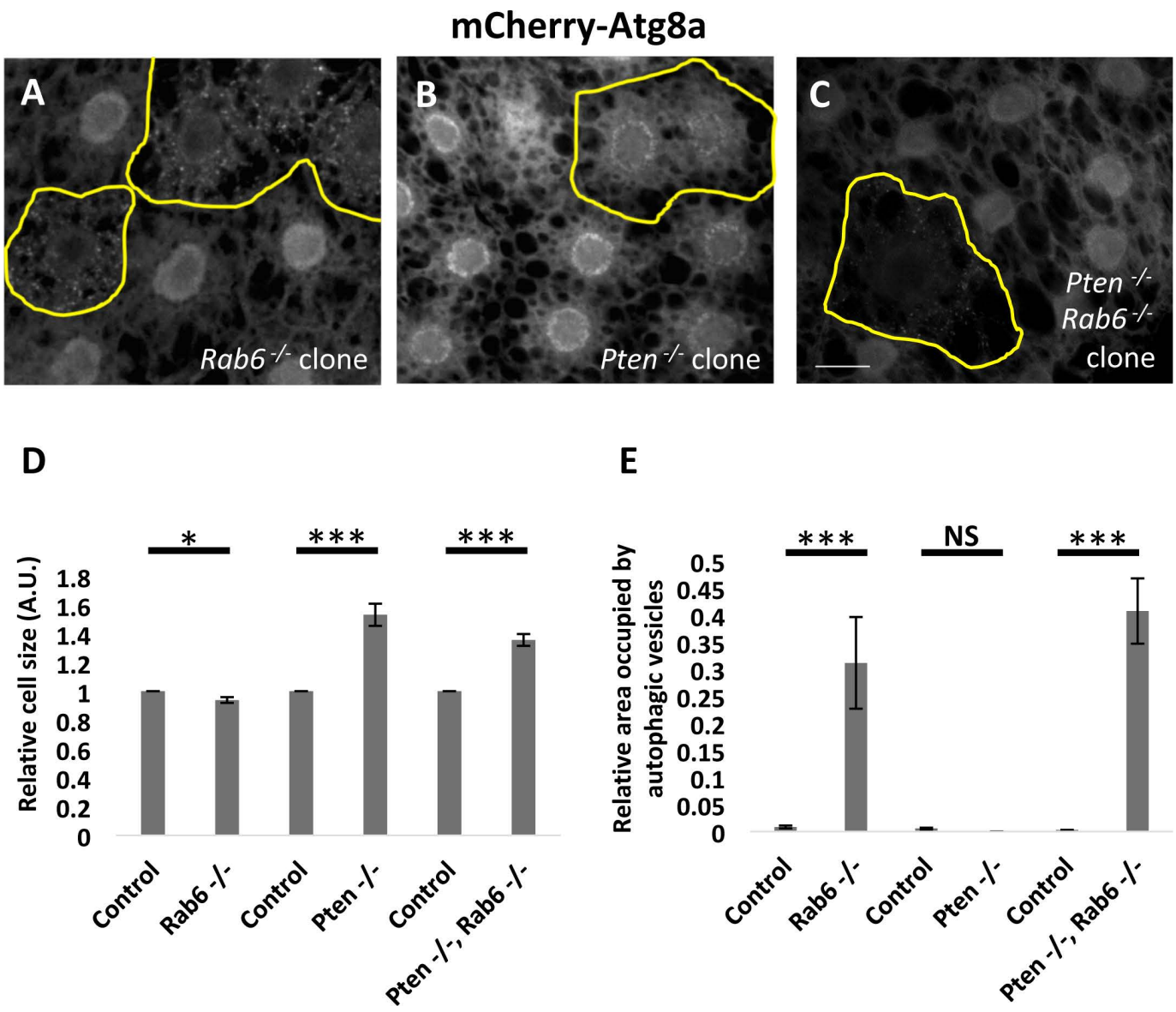

Figure S5. Cell size reduction in Rab6 null clones is rescued by deficiency of Pten.

A-C) Evaluation of mCherry-Atg8a marked autophagic vesicles under fed conditions in surrounding control cells and in *Rab6*$^{-/-}$ (A), *Pten*$^{-/-}$ (B), and *Rab6*$^{-/-}$ *Pten*$^{-/-}$ mutant clones (C).

D,E) Relative cell size and percent area occupied by mCherry-Atg8a punctae (each normalized to surrounding control cells) are indicated for the genotypes shown in in A-C.

Scalebar, 25 µm. Genotypes: A) *hs-flp; Rab6*^{D23D}*, FRT40A /UAS-2x-eGFP, FRT40A, fb-Gal4; UAS-mCherry-Atg8a/+.* B) *hs-flp; Pten*^{Dj189}*, FRT40A /UAS-2x-eGFP, FRT40A, fb-Gal4; UAS-mCherry-Atg8a/+.* C) *hs-flp; Rab6*^{D23D} *Pten*^{Dj189}*, FRT40A /UAS-2x-eGFP, FRT40A, fb-Gal4; UAS-mCherry-Atg8a/+.* N=10 larvae and 60 (A), 21 (B), 89 (C) clones analyzed per genotype. *p<0.05, ***p<0.01, NS p>0.05; Student's t-test. Error bars indicate s.e.m.

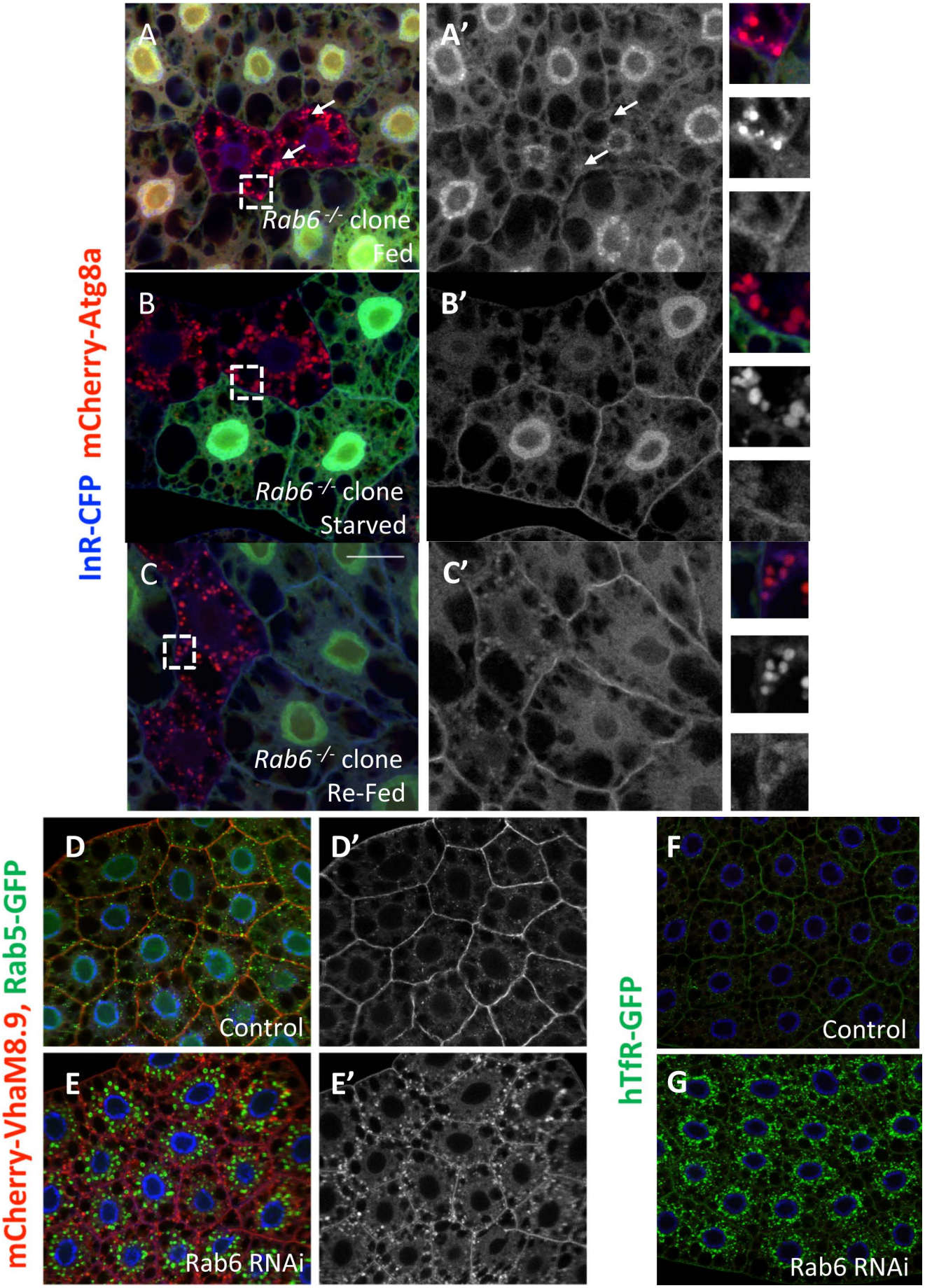
InR-CFP mCherry-Atg8a
A
A'
Rab6 -/- clone
Fed
B
B'
Rab6 -/- clone
Starved
C
C'
Rab6 -/- clone
Re-Fed
mCherry-VhaM8.9, Rab5-GFP
D
D'
Control
E
E'
Rab6 RNAi
hTfR-GFP
F
Control
G
Rab6 RNAi

Figure S6. Loss of Rab6 results in internalization of the insulin receptor independent of nutrient status and mis-localization of plasma membrane proteins.

A-C) Evaluation of mCherry-Atg8a marked autophagic vesicles and InR-CFP under basal states, starvation and full nutrient re-feeding in surrounding control cells and in *Rab6*$^{-/-}$ clones (marked by the absence of GFP). Blue channel (InR-CFP) for the distinct nutrient conditions is shown in grayscale in A', B' and C'. Insets show increased magnification of merge (top; Atg8a in red and InR-CFP in blue), mCherry-Atg8a (middle) and InR-CFP (bottom).

D-E) Depletion of Rab6 throughout the larval fat body results in expansion of the Rab5-GFP-marked early endosomal and VhaM8.9-mCherry late endosomal compartments (E) compared to control tissue (D); loss of plasma membrane localization of VhaM8.9 is also seen in Rab6 depleted tissue (E). D',E') depict red channel (mCherry-VhaM8.9) for better visualization. Fed conditions.

F-G) Depletion of Rab6 throughout the larval fat body results in expansion of the human Transferrin Receptor (hTfR)-GFP-marked recycling endosomal compartment (G) compared to control tissue (F). Fed conditions.

Scalebar, 25 µm. Genotypes: A-C) *hs-flp; Rab6*^{D23D}*, FRT40A /UAS-2x-eGFP, FRT40A, fb-Gal4; UAS-mCherry-Atg8a/UAS-InR-CFP.* D) *Cg-Gal4, UAS-mCherry-VhaM8.9/+; UAS-Rab5-GFP/+. E) Cg-Gal4, UAS-mCherry-VhaM8.9/+; UAS-Rab5-GFP/UAS-Rab6-dsRNA F) Cg-Gal4/+; UAS-hTfR-GFP/+. G) Cg-Gal4/+; UAS-hTfR-GFP/UAS-Rab6-dsRNA*

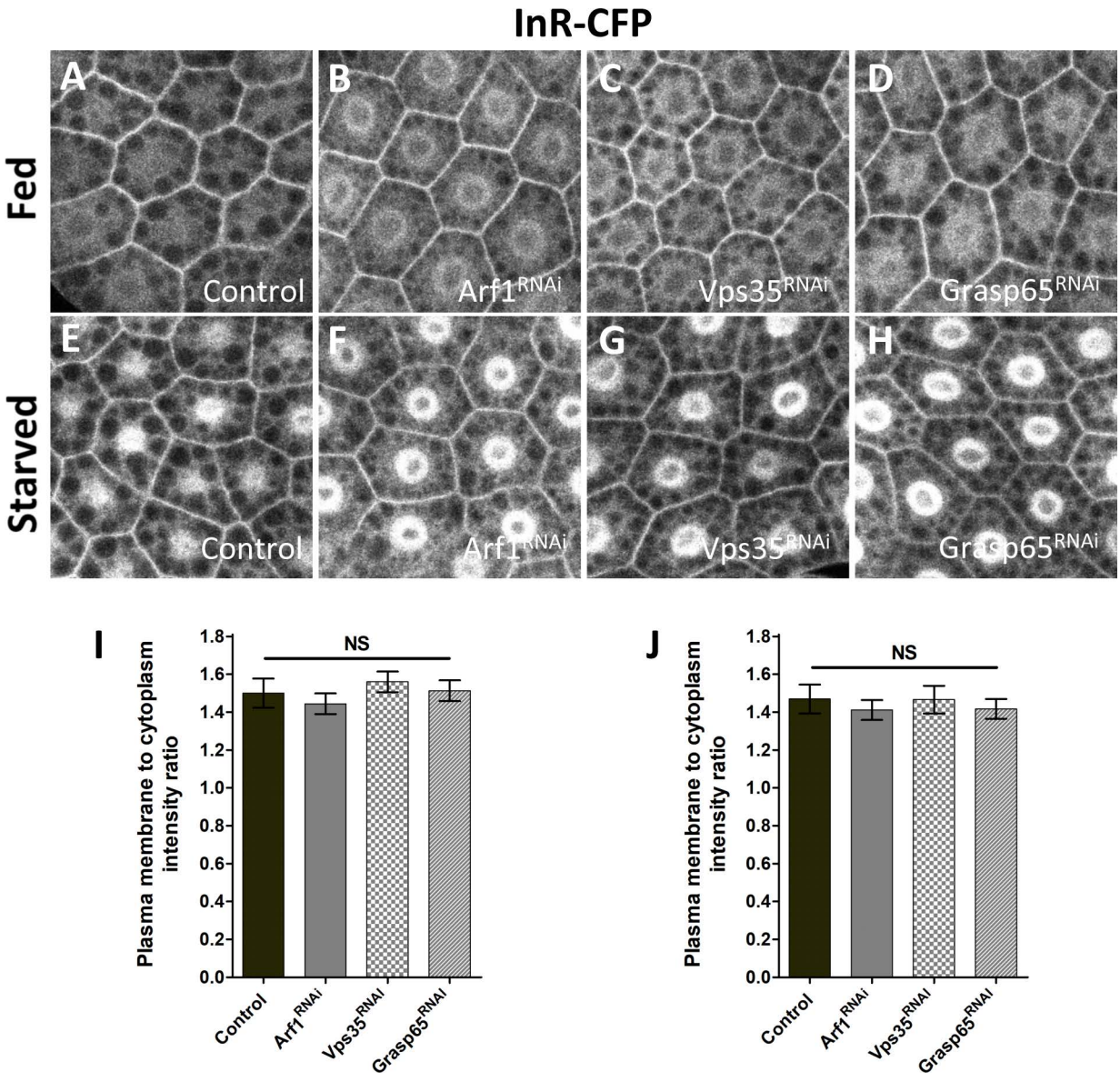

Figure S7. Effect of Golgi-associated protein depletion on InR localization.

Representative images of InR-CFP are shown in grayscale for control (A, E), Arf1- (B, F), Vps35- (C, G) and GRASP-65-depleted (D, H) fat body cells under fed and 4-hr starvation conditions as indicated. Quantified ratio of plasma membrane to cytoplasmic InR-CFP signal is shown in I (fed) and J (starved). n=10 larvae and 20 cells analyzed per condition and genotype. NS, p>0.05; Student's t-test. Error bars indicate s.e.m.

Genotypes: A, E) *Cg-Gal4/+; UAS-InR-CFP/+*. B, F) *Cg-Gal4/+; UAS-Arf1-dsRNA/UAS-InR-CFP*. C, G) *Cg-Gal4/+; UAS-Vps35-dsRNA/UAS-InR-CFP*. D, H) *Cg-Gal4/+; UAS-GRASP65-dsRNA/UAS-InR-CFP*.